

Testing Noncollinear Spin-Flip, Collinear Spin-Flip, and Conventional Time-Dependent Density Functional Theory for Predicting Electronic Excitation Energies of Closed-Shell Atoms

Xuefei Xu, Ke R. Yang, and Donald G. Truhlar*

Department of Chemistry and Supercomputing Institute, University of Minnesota, Minneapolis, Minnesota 55455, United States

S Supporting Information

ABSTRACT: Conventional time-dependent density functional theory (TDDFT) is based on a closed-shell Kohn–Sham (KS) singlet ground state with the adiabatic approximation, using either linear response (KS-LR) or the Tamm–Dancoff approximation (KS-TDA); these methods can only directly predict singly excited states. This deficiency can be overcome by using a triplet state as the reference in the KS-TDA approximation and “exciting” the singlet by a spin flip (SF) from the triplet; this is the method suggested by Krylov and co-workers, and we abbreviate this procedure as SF-KS-TDA. SF-KS-TDA can be applied either with the original collinear kernel of Krylov and co-workers or with a noncollinear kernel, as suggested by Wang and Ziegler. The SF-KS-TDA method does bring some new practical difficulties into play, but it can at least formally model doubly excited states and states with double-excitation character, so it might be more useful than conventional TDDFT (both KS-LR and KS-TDA) for photochemistry if these additional difficulties can be surmounted and if it is accurate with existing approximate exchange–correlation functionals. In the present work, we carried out calculations specifically designed to understand better the accuracy and limitations of the conventional TDDFT and SF-KS-TDA methods; we did this by studying closed-shell atoms and closed-shell monatomic cations because they provide a simple but challenging testing ground for what we might expect in studying the photochemistry of molecules with closed-shell ground states. To test their accuracy, we applied conventional KS-LR and KS-TDA and 18 versions of SF-KS-TDA (nine collinear and nine noncollinear) to the same set of vertical excitation energies (including both Rydberg and valence excitations) of Be, B⁺, Ne, Na⁺, Mg, and Al⁺. We did this for 10 exchange–correlation functionals of various types, both local and nonlocal. We found that the GVVNS and M06 functionals with nonlocal kernels in spin-flip calculations can both have accuracy competitive to CASPT2 calculations. When the results were averaged over all 36 test energy differences, seven (GVVNS, M06, B3PW91, LRC- ω PBE, LRC- ω PBEh, PBE, and M06-2X) of the 10 studied density functionals had smaller mean unsigned errors for noncollinear calculations than the mean unsigned error of the best functional (M06-2X) for either conventional KS-TDA or KS-LR.



1. INTRODUCTION

Time-dependent density functional theory¹ (TDDFT) is usually used with Kohn–Sham (KS) reference states in the linear response (LR) approximation² with the adiabatic approximation for the exchange–correlation functional; we abbreviate this as KS-LR. The adiabatic approximation in this context means using ground-state, frequency-independent approximate exchange–correlation functionals. The present article is entirely focused on using KS theory with the adiabatic approximation to predict electronic excitation energies, but we shall not restrict ourselves to the KS-LR approximation.

KS-LR has been widely tested for spectroscopy,³ especially vertical excitation energies, but much less attention has been devoted to calculating potential energy surfaces for photochemistry, although interest in the latter is increasing.^{4–9} A key consideration when one considers photochemistry is that KS-LR suffers from instabilities when the HOMO and LUMO are nearly degenerate.⁵ The Tamm–Dancoff approximation¹⁰ to KS-LR, which may be called KS-TDA, ameliorates these instabilities,⁵ as may be understood from its close similarity to

the variationally stable configuration interaction singles (CIS)¹¹ approximation of wave function theory. (CIS is the same as HF-TDA, where HF denotes a Hartree–Fock ground state.)

Conventional TDDFT (including both KS-LR and KS-TDA) is based on a closed-shell singlet ground state (and conventional TDDFT may therefore be called ground-state TDDFT). As a consequence, conventional TDDFT with the adiabatic approximation can only directly predict singly excited states. Ground-state KS-TDA fails to correctly predict the topography of the ground- and excited-state potential energy surfaces near a conical intersection in that, like CIS, it predicts an intersection in $F - 1$ degrees of freedom rather than the correct $F - 2$ degrees of freedom (where F is the full number of internal degrees of freedom),¹² although a configuration-interaction-corrected form of KS-TDA does correctly predict the topography of conical intersections.¹³ (It should be noted, however, that both CIS and KS-TDA are able to represent

Received: February 13, 2014

Published: April 1, 2014

conical intersections between two excited states.) Ground singlet–excited singlet conical intersections will be called S_0 – S_1 conical intersections.

The precise role of doubly excited states in molecular spectroscopy is complicated, maybe even controversial. However, a key point is that configuration interaction wave functions for both ground and excited states can contain significant contributions from states that are nominally of double-excitation character,¹⁴ and it may be advantageous to use a method of calculation in which these are explicitly included.

The incorrect modeling of S_0 – S_1 conical intersections and the inability to model doubly excited states can both be overcome by using a triplet state as the reference;¹⁵ this is called spin-flip (SF) TDDFT. We will apply this theory with the Tamm–Dancoff approximation and abbreviate it as SF-KS-TDA. This procedure does bring some new practical difficulties into play, but we found that it is not unstable near conical intersections, and because SF can at least formally model S_0 – S_1 conical intersections and doubly excited states, it might be more useful than ground-state KS-TDA for photochemistry if these additional difficulties can be surmounted and if it is accurate with existing approximate exchange–correlation functionals. The present article is concerned with this latter issue—accuracy.

Although the motivation for studying spin-flip methods comes from molecular spectroscopy and photochemistry, in the present article we propose to try to understand its accuracy and limitations better by studying closed-shell atoms and closed-shell monatomic cations in particular because they provide a simple testing ground for what we might expect in studying the photochemistry of molecules with closed-shell ground states. One advantage of studying atoms is that they eliminate the complications of charge-transfer excitation, left–right correlation energy, Franck–Condon factors, and experimental resolution, which complicate studies of molecules. Another advantage is that valence and Rydberg states are neatly separated, whereas in molecules they are often mixed, complicating one's ability to see trends. In particular, then, we applied KS-LR, KS-TDA, and 18 schemes of SF-KS-TDA (nine collinear¹⁵ and nine noncollinear¹⁶) to the same set of vertical excitation energies (including both Rydberg and valence excitations) of Be, B^+ , Ne, Na^+ , Mg, and Al^+ to test their accuracy. We carried out these tests for 10 exchange–correlation functionals of various kinds.

2. THEORY

2.1. Conventional KS-LR and KS-TDA. TDDFT is an extension of KS theory into the time domain, with the two Runge–Gross¹ theorems (RG1 and RG2) as its formal foundation.^{1,4,8,17} RG1 and RG2 are analogous to the two Hohenberg–Kohn theorems¹⁸ (HK1 and HK2, respectively) of the original ground-state DFT. On the basis of RG1, the external potential is determined, up to an additive function of time, by the time-dependent charge density and the initial ground-state wave function $\Psi_0 = \Psi(t = t_0)$, so the time-dependent KS equations for the orbitals ψ_p become

$$\left[-\frac{1}{2}\nabla_1^2 + v_{\text{ext}}(r_1, t) + \int \frac{\rho(r_2, t)}{r_{12}} dr_2 + v_{\text{xc}}[\rho(r_1, t)] \right] \times \psi_p(r_1, t) = i \frac{\partial \psi_p(r_1, t)}{\partial t} \quad (1)$$

where $-\frac{1}{2}\nabla_1^2$ is the electron kinetic energy operator, v_{ext} is the time-dependent external potential, ρ is the electron density, $\int [\rho(r_2, t)/r_{12}] dr_2$ is the classical electron–electron Coulomb repulsion, and v_{xc} is the time-dependent exchange–correlation potential. RG2 was initially based on a stationary action principle analogous to the variational principle of the second Hohenberg–Kohn theorem HK2 with the Dirac–Frenkel action. This theorem was improved by using a more appropriate Keldysh action formalism.¹⁹

The calculation of excited states is the main application of the time-dependent KS equation. Applying a time-dependent perturbation (e.g., a time-dependent electric field) to an N -electron system that is initially in its ground stationary state and deducing an equation for the dynamic linear response of the KS density matrix, one obtains the KS-LR eigenvalue equation:²

$$\begin{bmatrix} \mathbf{A} & \mathbf{B} \\ \mathbf{B}^* & \mathbf{A}^* \end{bmatrix} \begin{bmatrix} \mathbf{Y} \\ \mathbf{Z} \end{bmatrix} = (E_1 - E_0) \begin{bmatrix} \mathbf{I} & 0 \\ 0 & -\mathbf{I} \end{bmatrix} \begin{bmatrix} \mathbf{Y} \\ \mathbf{Z} \end{bmatrix} \quad (2)$$

where \mathbf{I} denotes a unit matrix, $(E_1 - E_0)$ is the excitation energy,

$$A_{ia,jb} = \delta_{ij}\delta_{ab}(\epsilon_a - \epsilon_i) + (ialjb) - \frac{X}{100}(ijlab) + \left(1 - \frac{X}{100}\right)(ialf_{\text{xc}}ljb) \quad (3)$$

and

$$B_{ia,bj} = (ialbj) - \frac{X}{100}(iblabj) + \left(1 - \frac{X}{100}\right)(ialf_{\text{xc}}lbj) \quad (4)$$

in which

$$(ialjb) = \int dr_1 dr_2 \phi_i(r_1)\phi_a(r_1)\frac{1}{r_{12}}\phi_b(r_2)\phi_j(r_2) \quad (5)$$

and

$$(ialf_{\text{xc}}ljb) = \int dr_1 dr_2 \phi_i(r_1)\phi_a(r_1)\frac{\delta^2 E_{\text{xc}}(\rho)}{\delta\rho(r_1)\delta\rho(r_2)}\phi_b(r_2)\phi_j(r_2) \quad (6)$$

where i, j, \dots label occupied spin-orbitals and a, b, \dots label unoccupied orbitals. For conventional TDDFT calculations, the spin-orbitals are generated by restricted KS (RKS) self-consistent-field (SCF) calculations on the ground state. In the above equations, $A_{ia,jb}$ is the element of matrix \mathbf{A} coupling two one-electron excitations $i \rightarrow a$ and $j \rightarrow b$, $B_{ia,bj}$ is the element of matrix \mathbf{B} coupling an $i \rightarrow a$ excitation to a $j \leftarrow b$ de-excitation, $\epsilon_a - \epsilon_i$ is the molecular orbital energy difference of spin-orbitals a and i , X is the percentage of Hartree–Fock exchange in the exchange–correlation functional, f_{xc} is called the kernel and is the functional derivative of the exchange–correlation potential, and eqs 5 and 6 are a two-electron repulsion integral and the response of the exchange–correlation potential, respectively.

Thus, by carrying out a ground-state calculation and solving eq 2, one can obtain the excitation energy $E_1 - E_0$ by KS-LR. Since we know E_0 from the ground-state SCF calculation, this yields the energy E_1 of the excited state.

The matrix \mathbf{B} in KS-LR is a measure of the missing correlation in the ground state, but since DFT already includes correlation in the ground state through the use of an exchange–correlation functional, it is not unreasonable to introduce the Tamm–Dancoff approximation (TDA) to

TDDFT by neglecting the matrix B .¹⁰ The KS-TDA eigenvalue equation is then given by

$$AY = (E_1 - E_0)Y \quad (7)$$

2.2. SF-KS-TDA. In SF-KS-TDA,¹⁵ one begins with an unrestricted Kohn–Sham (UKS) SCF calculation (sometimes called a spin-polarized calculation) of triplet state T_j , whose density is represented by the Slater determinant

$$\Psi(T_j) = |(\text{core})\phi_p\alpha\phi_q\alpha| \quad (8)$$

which has total electron spin component $M_S = +1$. The spin-flip “excitation” process, which can be either an excitation or a de-excitation from an α spin-orbital to a β spin-orbital, generates $M_S = 0$ states, and the energies of the spin-flip states are calculated using the TDA. The states that are generated in this way are not necessarily eigenfunctions of \hat{S}^2 , where S is the total spin. (Nor are the UKS initial determinants eigenfunctions of \hat{S}^2 because the variationally best determinant of the form of eq 8 has different orbitals for different spins in the core. We should keep in mind that \hat{S}^2 is a two-electron operator, and even if a theory yields the correct one-particle density and the correct energy, it is not guaranteed to yield the correct expectation value of \hat{S}^2 .)

When a collinear kernel is used in the matrix A (i.e., when each spin-orbital is required to have either α or β spin but not some linear combination of the two), both eqs 5 and 6 are zero because orbitals i and a always have opposite spin, and j and b as well. Therefore, only the Hartree–Fock exchange contributes to off-diagonal elements of A in collinear SF-KS-TDA calculations. For a local exchange–correlation functional [such as the local spin density approximation (LSDA), a generalized gradient approximation (GGA), or a meta-GGA], the excitation energy calculated by SF-KS-TDA with a collinear kernel equals the orbital energy difference $\epsilon_a - \epsilon_i$. This is not an accurate estimate of excitation energies, and therefore, a high X is usually required for SF-KS-TDA with a collinear kernel to obtain good agreement with experiments.

SF-KS-TDA is more accurate with local functionals if one uses a noncollinear representation^{20–22} of the exchange–correlation potential, where the α and β spin-orbitals are allowed to mix together. In the present work, we used Wang and Ziegler’s¹⁶ reformulation of SF-TDDFT with noncollinear kernels. (Noncollinear kernels were originally proposed by Liu and co-workers^{21,23} for relativistic TDDFT.) In noncollinear SF-KS-TDA, a collinear Slater determinant is still used for the reference triplet state.

2.3. Spin Contamination Introduced by SF-KS. As shown in Figure 1, excitations from the reference triplet state determinant (a) that involve a spin flip can generate singly excited determinants b – j . The closed-shell determinants b and c are always eigenfunctions of \hat{S}^2 , and they correspond to the singlet ground state and its doubly excited determinant in the open-shell subspace of the reference triplet state, respectively. The generation of configurations like c is how SF-KS can handle double excitations with multireference character. However, the other singly excited determinants in Figure 1 are the source of the main problem in the SF scheme, namely, spin contamination due to singlet–triplet mixing and spin incompleteness.²⁴ The determinants d – j are not spin eigenfunctions, but d and e are spin counterparts of each other and thus can be linearly combined to obtain the eigenfunctions of \hat{S}^2 ; the positive and negative combinations of

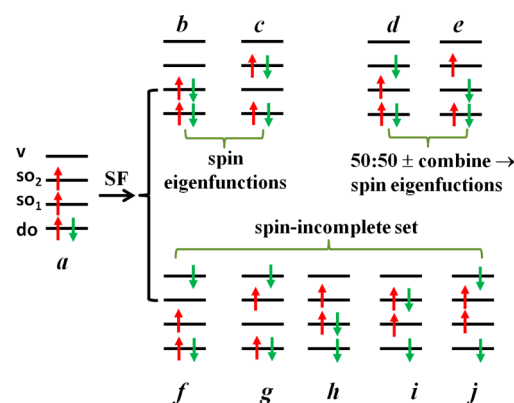


Figure 1. Reference determinant a and the determinants b – j obtained by spin-flip excitations. In this figure, do, so, and v denote doubly occupied orbitals, singly occupied orbitals, and virtual orbitals.

d and e yield triplet and open-shell singlet \hat{S}^2 eigenfunctions, respectively. However, sometimes the SF-KS calculations still suffer singlet–triplet mixing involving these two determinants, and one obtains a spin-contaminated state with $\langle S^2 \rangle \approx 1$ [if one had a precisely 50:50 mixture of singlet (with $\langle S^2 \rangle = 0$) and the corresponding triplet (with $\langle S^2 \rangle = 2$), one would have $\langle S^2 \rangle$ precisely, rather than approximately, equal to 1]. The spin counterparts of f – j are missing in the single excitation of the reference state a , so any states involving these determinants are seriously spin-contaminated, with $\langle S^2 \rangle \approx 1$.

In one of our recent papers,⁹ we proposed the use of Yamaguchi’s approximate spin projection formula²⁵ to cancel the spin contamination introduced by this spin incompleteness. The energy of an open-shell singlet state is then calculated as

$$E_S = E_T - \frac{2(E_T - E_{\text{mix}})}{\langle S^2 \rangle_T - \langle S^2 \rangle_{\text{mix}}} \quad (9)$$

where E_T in eq 9 is the energy of the triplet reference state obtained from the unrestricted KS calculations and $\langle S^2 \rangle_T$ and $\langle S^2 \rangle_{\text{mix}}$ are the expectation values for the triplet reference state and the spin-mixed state with energy E_{mix} obtained from the SF-KS calculations, respectively. The resulting singlet energy E_S is labeled as SF-KS-Y, where Y denotes use of the Yamaguchi approximate projection formula (eq 9). In previous publications, we have sometimes called this the weighted-average broken-symmetry (WABS) method because eq 9 can be rewritten as a weighted average of E_T and E_{mix} :

$$E_S = \frac{\Delta - 2}{\Delta} E_T + \frac{2}{\Delta} E_{\text{mix}} \quad (10)$$

where

$$\Delta = \langle S^2 \rangle_T - \langle S^2 \rangle_{\text{mix}} \quad (11)$$

This method is in principle useful only for the spin contamination introduced by singlet–triplet mixing involving only determinants d and e , which have the same singly occupied spatial orbitals as the reference triplet. It is not really appropriate for spin-contaminated states involving determinants f – j . The states one actually gets are mixtures of both kinds of determinants, and the determinant that dominates the mixture depends on the system, the exchange–correlation functional, and the basis set; therefore, it is not always obvious whether the formula is applicable. We tested schemes where it is applied and schemes where it is not.

Table 1. Atoms and Cations Used for Testing, Their Dominant Electron Configurations in Each of the Four Excited States Considered, and the Experimental Excitation Energies²⁶ (in eV)

	T ₁		S ₁		T ₂		S ₂		Splitting	
	conf.	T ₁ – S ₀	conf.	S ₁ – S ₀	conf.	T ₂ – S ₀	conf.	S ₂ – S ₀	S ₁ – T ₁	S ₂ – T ₂
Be	2s2p	2.73	2s2p	5.28	2s3s	6.46	2s3s	6.78	2.55	0.32
B ⁺	2s2p	4.63	2s2p	9.10	2s3s	16.09	2s3s	17.06	4.47	0.97
Ne	2p ⁵ 3s	16.65	2p ⁵ 3s	16.85	2p ⁵ 3p	18.58	2p ⁵ 3p	18.74	0.20	0.16
Na ⁺	2p ⁵ 3s	32.90	2p ⁵ 3s	33.32	2p ⁵ 3p	36.92	2p ⁵ 3p	37.35	0.43	0.43
Mg	3s3p	2.71	3s3p	4.35	3s4s	5.11	3s4s	5.39	1.63	0.29
Al ⁺	3s3p	4.65	3s3p	7.42	3s4s	11.32	3s4s	11.82	2.77	0.51

3. SYSTEMS AND STATES STUDIED

In the present work, we applied conventional KS-LR and KS-TDA along with 18 schemes of SF-KS-TDA (nine collinear and nine noncollinear) to investigate the two triplet states and two excited singlet states and their singlet–triplet splitting for six closed-shell monatomic systems, namely, Be, B⁺, Ne, Na⁺, Mg, and Al⁺. We label the closed-shell ground state as S₀ and the considered excited states as T₁, T₂, S₁, and S₂, where the state with subscript 2 is higher in energy than the one with subscript 1 for the same spin but the 1 and the 2 do not necessarily mean that they are the first and second triplet or first and second excited singlet state for that system. The electron configurations, the experimental²⁶ excitation energies of these states relative to their ground state S₀, and the singlet–triplet splittings are listed in Table 1.

For each system and each method, we calculated six values: two triplet excitation energies (T₁ – S₀ and T₂ – S₀), two singlet excitation energies (S₁ – S₀ and S₂ – S₀), and two spin splittings (S₁ – T₁ and S₂ – T₂) of a singlet and a triplet with same configurations. We also calculated their signed and unsigned errors relative to the experimental data.

4. DENSITY FUNCTIONALS TESTED

Ten exchange–correlation functionals were tested: (1) GVVNS,²⁷ an example of an LSDA functional, which depends only on local spin densities ρ_{σ} ; (2) PBE,²⁸ an example of a GGA that depends not only on the local ρ_{σ} values but also on their reduced gradient s^2 ; (3, 4) two global-hybrid GGAs, B3PW91²⁹ and B97-1,³⁰ which are functionals where a percentage X of local exchange is replaced by Hartree–Fock exchange, where X is a global constant; (5–7) three long-range-corrected (LRC) functionals, in which X increases as a function of interelectronic separation to correct the incorrect asymptotic behavior of the exchange–correlation potential: LRC- ω PBE^{31,32} ($\omega = 0.3a_0^{-1}$), LRC- ω PBEh³² ($\omega = 0.2a_0^{-1}$), and ω B97X³³ ($\omega = 0.3a_0^{-1}$), where ω is the optimized value of the range-separation parameter; and (8–10) three M06-series functionals: the meta-GGA M06-L³⁴ (a meta-GGA is like a GGA but also depends on local values of the spin-labeled kinetic energy densities τ_{α} and τ_{β}) and two global-hybrid meta-GGAs, M06^{35,36} and M06-2X,^{35,36} which are hybrid meta-GGAs where the percentage X of local exchange replaced by Hartree–Fock exchange is a global constant. The percentage of Hartree–Fock exchange X for each functional is listed in Table 2.

Why were these functionals chosen? GVVNS, PBE, M06-L, and B3PW91 are well-established functionals that are reasonably representative of successful functionals in their respective classes of LSDA, GGA, meta-GGA, and global-hybrid GGA. B97-1 provides an alternative in the global-hybrid

Table 2. Exchange–Correlation Functionals Tested in This Work

functional ^a	type	X ^b	ref(s)
GVVNS ^c	LSDA	0	27
PBE	GGA	0	28
M06-L	meta-GGA	0	34
LRC- ω PBE	long-range-corrected GGA	0–100	31, 32
ω B97X	long-range-corrected GGA	15.77–100	33
B3PW91	global-hybrid GGA	20	29
LRC- ω PBEh	long-range-corrected GGA	20–100	32
B97-1	global-hybrid GGA	21	30
M06	global-hybrid meta-GGA	27	35, 36
M06-2X	global-hybrid meta-GGA	54	35, 36

^aAcronyms: GVVNS: Gáspár exchange with Vosko–Wilk–Nusiar no. 5 correlation; PBE: Perdew–Burke–Ernzerhof; M06-L: Minnesota 2006 local; LRC- ω PBE: long-range-corrected PBE with range parameter ω ; B3PW91: Becke three-parameter functional with Perdew–Wang 1991 correlation; LRC- ω PBEh: like LRC- ω PBE but modified by Rohrdanz et al.;³² B97-1: the first functional of Hamprecht, Cohen, Tozer, and Handy (published in the same paper as HCTH/93) using the Becke 1997 functional form; M06: Minnesota 2006; M06-2X: M06 with twice as much Hartree–Fock exchange (X) as M06. ^bX is the percentage of Hartree–Fock exchange; since we used local correlation functionals in this article, functionals with X = 0 are local, and only those with X > 0 are nonlocal. When a range is given for X, the first value is the percentage in the limit $r \rightarrow 0$, where r is the interelectronic distance, and the second value is the percentage in the limit $r \rightarrow \infty$. ^cGVVNS is called SVVNS in *Gaussian 09*, where S denotes renormalized Slater. GVVNS employs the Gáspár exchange functional, which is smaller than the one derived by Slater by a factor of 2/3; the Gáspár exchange functional was also employed in the original Kohn–Sham paper.

GGA class that was chosen because of its outstanding performance in tests^{37,38} of functionals for metal–ligand bond energies of 3d transition metals. M06 and M06-2X were chosen because of generally good performance on a large number of tests against various ground-state and excited-state data^{3,35,39–43} and in a variety of applications. LRC- ω PBEh was shown to perform well for ground-state atomization energies, valence excitation energies in both small- and medium-sized molecules, and charge-transfer excitations, and LRC- ω PBE was found to have comparable performance for localized and charge-transfer excitations, although it performs more poorly for atomization energies.³² Finally, ω B97X was chosen as a long-range-corrected functional having a form very similar to that of LRC- ω PBEh but predating it.

5. COMPUTATIONAL DETAILS

For KS-LR and KS-TDA, which use the closed-shell ground state (S₀) as the reference, each excitation energy was obtained

Table 3. Nine Schemes for either Collinear or Noncollinear SF-KS-TDA^{a,b}

scheme	S ₀	S ₁	S ₂	T ₁ and T ₂
I11	SF unprojected with T ₁ as the reference	SF unprojected with T ₁ as the reference	SF unprojected with T ₁ as the reference	UKS
S11	RKS	SF unprojected with T ₁ as the reference	SF unprojected with T ₁ as the reference	UKS
222	SF unprojected with T ₂ as the reference	SF unprojected with T ₂ as the reference	SF unprojected with T ₂ as the reference	UKS
S22	RKS	SF unprojected with T ₂ as the reference	SF unprojected with T ₂ as the reference	UKS
SPQ	RKS	SF projected with T ₁ as the reference	SF projected with T ₂ as the reference	UKS
SPP	RKS	SF projected with T ₁ as the reference	SF projected with T ₁ as the reference	UKS
SQQ	RKS	SF projected with T ₂ as the reference	SF projected with T ₂ as the reference	UKS
M12	SF unprojected with T ₁ or T ₂ as the reference	SF unprojected with T ₁ as the reference	SF unprojected with T ₂ as the reference	UKS
S12	RKS	SF unprojected with T ₁ as the reference	SF unprojected with T ₂ as the reference	UKS

^aS₀ is the ground singlet state; T₁ and S₁ are the lower-energy triplet and singlet states, respectively; T₂ and S₂ are the higher-energy triplet and singlet states, respectively. ^b“SF projected” means that the energies were corrected using Yamaguchi’s formula (eq 9).

as the difference of the absolute energy of the excited state obtained by corresponding TDDFT calculations and the absolute energy of S₀ obtained by restricted KS calculations. For SF-KS-TDA with either a collinear or noncollinear kernel, the precise way to calculate the excitation energies is not so clear. For each kind of kernel, nine schemes were tested, as explained next (a summary, which may be useful to consult while reading the explanation, is given in Table 3).

The first consideration, applicable to all nine schemes, is that in the present study the SF-KS-TDA method was used only to obtain the energies of singlet states, since open-shell triplet states usually can be well-represented and accurately calculated by the UKS method, whereas in most SF-KS-TDA calculations, the triplet states show significant spin contamination. Thus, for calculations of the six values T₁ – S₀, T₂ – S₀, S₁ – S₀, S₂ – S₀, S₁ – T₁, and S₂ – T₂ for all nine schemes of each kind of kernel, the energies of T₁ and T₂ were obtained by UKS. However, for the closed-shell ground state (determinant *b* in Figure 1), we used two different methods. Although SF-KS-TDA calculations tend to yield less spin contamination for the ground state than for excited singlet states, the orbitals used in SF-KS-TDA are optimized for the triplet reference state rather than for the ground state, so the energy of the S₀ state calculated by SF-KS-TDA is less accurate than that obtained by a restricted KS calculation. Therefore, for the S₀ energy, we considered both the RKS and the SF methods. In addition, we used different triplet states as references in the SF-KS-TDA calculations. We also tested the performance of projected SF-KS-TDA calculations using Yamaguchi’s approximate spin projection formula (eq 9). Combining these steps in various ways yields schemes that may be denoted XYZ (see Table 3), where X, Y, and Z denote the procedures for calculating S₀, S₁, and S₂, respectively. The single-character abbreviations for the various schemes are as follows:

- S: The absolute energy of S₀ is from an RKS calculation.
- 1: The absolute energy of a singlet state is obtained from unprojected SF-KS-TDA calculations using T₁ as the reference.
- 2: The absolute energy of a singlet state is obtained from unprojected SF-KS-TDA calculations using T₂ as the reference.
- P: The absolute energy of an excited singlet state is obtained from SF-KS-Y calculations using T₁ as the reference.
- Q: The absolute energy of an excited singlet state is obtained from SF-KS-Y calculations using T₂ as the reference.

M: In the excitation energy calculations for S₁ or T₁, the energy of S₀ is obtained from unprojected SF-KS-TDA calculations using T₁ as the reference, and in the excitation energy calculations for S₂ or T₂, the energy of S₀ is obtained from unprojected SF-KS-TDA calculations using T₂ as the reference.

Combining these in various ways yields the nine schemes tested, as summarized in Table 3.

6. STATE ASSIGNMENTS

The next issue of concern is assigning the states resulting from an SF-KS-TDA calculation, since this is not always obvious. As we mentioned above, the closed-shell S₀ state is a pure singlet spin state and can be described by SF-KS-TDA with small spin contamination. Therefore, we can identify it in SF-KS-TDA output files by its character (the *b* determinant in Figure 1) plus the fact that its $\langle S^2 \rangle$ value is close to 0. However, assigning S₁ and S₂ states can be ambiguous, so we developed unambiguous rules rather than simply selecting the energies that agree best with experiment, since the latter option would not be available in real applications where an unknown spectrum is being predicted and also could involve fortuitously small errors from misassigned states. We believe that it is essential in testing of methods that each method should be defined unambiguously and not require decisions that might be made differently by different investigators; this “well-defined” aspect of a method is an essential prerequisite for defining what Pople⁴⁴ called a theoretical model chemistry.

In ideal situations, using T₁ (or T₂) as the reference, one obtains the pure S₁ (or S₂) state with $\langle S^2 \rangle = 0$ and the pure T₁ (or T₂) state with $\langle S^2 \rangle = 2$; these are obtained as the negative and positive 50:50 combinations of determinants *d* and *e* shown in Figure 1, and one also obtains the spin-mixed S₂–T₂ (or S₁–T₁) state with $\langle S^2 \rangle = 1$ because of the absence of a spin counterpart. However, in real situations, one finds that the pure singlet S₁ (or S₂) and triplet T₁ (or T₂) states obtained with T₁ (or T₂) as the reference very often mix, as shown in Figure 2

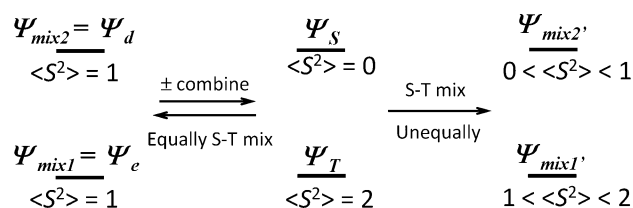


Figure 2. Singlet–triplet mixing.

Table 4. Assignments of the Excited Singlet State from the SF-KS-TDA Calculations

$\alpha \rightarrow \beta$ spin flip ^a	open-shell ^b	$\langle S^2 \rangle$	E (eV)	assignment
Be: Collinear SF-KS-TDA Calculation Using GVWN5 with the 2s2p _y Triplet State as the Reference				
2p _x → 2p _y	2s, 2p _y	1.0000	−388.6125	EA for the 2s2p singlet
2p _x → 2p _z	2s, 2p _z	1.0000	−388.6125	
2p _x → 2p _x	2s, 2p _x	1.0000	−388.2763	OA for the 2s2p singlet
2s → 2s	2s, 2p _x	1.0000	−388.0919	SA for the 2s2p singlet
2p _x → 3s	2s, 3s	0.9910	−387.4153	EA, OA, SA for the 2s3s singlet
Be: Noncollinear SF-KS-TDA Calculation Using GVWN5 with the 2s3s Triplet State as the Reference				
3s → 2p _y	2s, 2p _y	1.0000	−389.8622	EA,OA,SA for the 2s2p singlet
3s → 2p _z , 3s → 2p _x	2s, 2p _z or 2p _x	1.0000	−389.8622	
3s → 2p _z , 3s → 2p _x	2s, 2p _z or 2p _x	1.0000	−389.8622	
(2s → 2s) + (3s → 3s)	2s, 3s	2.0000	−387.0493	
(3s → 3s) − (2s → 2s)	2s, 3s	0.0155	−386.7037	EA,OA,SA for the 2s3s singlet
Ne: Noncollinear SF-KS-TDA Calculation Using LRC-ωPBEh with the 2p _x 2p _z 2p _y 3p _y Triplet as the Reference				
3p _y → 3s	2p _y , 3s	1.0012	−3489.8641	EA,OA,SA for the 2p ⁵ 3s singlet
2p _z → 2p _y	2p _z , 3p _y	1.0027	−3488.0106	EA for the 2p ⁵ 3p singlet
2p _x → 2p _y	2p _x , 3p _y	1.0027	−3488.0106	
2p _y → 2p _y	2p _y , 3p _y	1.2161	−3487.7078	OA for the 2p ⁵ 3p singlet
3p _y → 3p _x	2p _y , 3p _x	1.0012	−3487.3271	
3p _y → 3p _y	2p _y , 3p _y	0.7750	−3486.1590	SA for the 2p ⁵ 3p singlet

^aThe main excitation(s) contributing to the state obtained by spin-flip excitation from the reference triplet. ^bThe resulting open-shell orbitals.

(or we can say that the spin counterparts d and e are not combined well). An equal mixture of S_1 and T_1 (or S_2 and T_2) gives two spin non-eigenfunctions $\Psi_{\text{mix}2}$ and $\Psi_{\text{mix}1}$ (which are equal to Ψ_d and Ψ_e respectively) with $\langle S^2 \rangle = 1$ (left side of Figure 2), and unequal mixing leads to $\Psi_{\text{mix}2'}$ and $\Psi_{\text{mix}1'}$, which have $\langle S^2 \rangle$ values of 0–1 or 1–2 (right side of Figure 2). Which state energy should be taken as the energy of S_1 (or S_2)? We calculated three sets of results for the present SF-KS-TDA tests. For assignment method 1, we chose the lowest-energy state with S_1 (or S_2) configuration character as S_1 (or S_2) only if this state had $\langle S^2 \rangle = 0$ –1.5 (because we think that a state with $\langle S^2 \rangle > 1.5$ is more like a pure triplet state); otherwise, we chose another mixed state with a smaller $\langle S^2 \rangle$ value (0–0.5) but higher energy. Because we mainly assigned the excited singlet states on the basis of the energy in assignment method 1, we denote it as EA (“energy-based assignment”). For assignment methods 2 and 3, we chose the states whose main determinants were in the open-shell subspace of the reference triplet state for the singlet state with the same configuration character as the reference; for the singlet state with different configuration character from the reference, which always had $\langle S^2 \rangle \approx 1$, we just chose the state with the lowest energy. Such assignments avoid the spin contaminations to some extent because of the involvement of determinants f – j for the singlet state with the same configuration character as the reference. The difference between assignment methods 2 and 3 is that for assignment method 2, which we denote as OA (“occupation-based assignment”), we chose the lowest-energy state with the same singly occupied spatial orbitals as the reference only if this state had $\langle S^2 \rangle = 0$ –1.5, otherwise, we chose another mixed state with a smaller $\langle S^2 \rangle$ value (0–0.5) but higher energy. For assignment method 3, which we denote as SA (“spin-based assignment”), we always chose the state with the smallest $\langle S^2 \rangle$ value, and if the $\langle S^2 \rangle$ values of two states were very close to each other (e.g., the difference was smaller than 0.01), we chose the state with the higher energy. In subsection 9.1, we will take Be and Ne atoms as examples to illustrate in detail how we assigned the states using the three assignment methods.

7. BASIS SETS

As shown in Table 1, 16 of the 24 excitations from ground states considered in present work are Rydberg excitations, for which diffuse basis functions are important to obtain accurate results.^{45,46} For Be, B⁺, Mg, and Al⁺, we used the aug-cc-pVQZ^{47–49} basis set; for the noble gas Ne, which has a “full” valence electron shell, the doubly augmented polarized valence correlation-consistent quadruple- ζ basis set d-aug-cc-pVQZ⁴⁷ was used (double augmentation means twice as many diffuse functions for each orbital angular momentum); for Na⁺, the excitations tested here are the electronic excitations from the core shells of Na, so we used the augmented correlation-consistent polarized core–valence basis set aug-cc-pCVQZ,⁴⁹ which can adequately describe core and core–valence correlation effects.

8. WAVE FUNCTION CALCULATIONS FOR COMPARISON

For comparison, we also carried out TDHF,⁵⁰ CIS,⁵¹ spin-flip CIS (SF-CIS),⁵² CASPT2,⁵³ and EOM-CCSD⁵⁴ calculations on the same test set.

The CASPT2 calculations were based on state-averaged CASSCF calculations as reference states. Because of the degeneracies (e.g., triply degenerate 2s2p states) and occasional shifting of the order of the states, we averaged over ten singlet and ten triplet states in each case, except for the singlet states of Be for which we averaged over only five. In the CASPT2 calculations, in consideration of the excitations to be investigated, as shown in Table 1, the 2s orbital, the three 2p orbitals, and the 3s orbital were included in the active spaces of Be and B⁺; the three 2p orbitals, the 3s orbital, and the three 3p orbitals were chosen for the active spaces of Ne and Na⁺; and the 3s orbital, the three 3p orbitals, and the 4s orbital were selected as the active orbitals of Mg and Al⁺. Thus, the CASPT2 calculations involved 5–7 active orbitals per atom, which is larger than is often affordable for molecules, so the performance of CASPT2 in practical calculations on molecules might be slightly poorer.

Table 5. Values of MUE(60), MUEV(30), and MUER(30) (in eV) of SF-KS-TDA, KS-LR and KS-TDA for Be Averaged over 10 Functionals

assign.	scheme	collinear			noncollinear		
		MUE(60)	MUEV(30)	MUER(30)	MUE(60)	MUEV(30)	MUER(30)
Spin-Flip TDDFT (SF-KS-TDA)							
EA	111	5.35	5.30	5.40	1.80	1.70	1.90
EA	S11	0.91	0.90	0.93	0.62	0.68	0.56
EA	222	4.37	4.27	4.47	3.19	3.26	3.12
EA	S22	2.79	2.17	3.40	0.64	0.94	0.34
EA	SPQ	5.38	3.34	7.42	1.36	2.27	0.45
EA	SPP	2.50	3.34	1.67	1.53	2.27	0.78
EA	SQQ	6.45	5.48	7.42	1.56	2.67	0.45
EA	M12	4.88	5.30	4.47	2.41	1.70	3.12
EA	S12	2.15	0.90	3.40	0.51	0.68	0.34
OA	111	5.34	5.28	5.40	1.76	1.62	1.90
OA	S11	1.04	1.15	0.93	0.66	0.77	0.56
OA	222	4.37	4.27	4.47	3.19	3.26	3.12
OA	S22	2.79	2.17	3.40	0.64	0.94	0.34
OA	SPQ	5.63	3.85	7.42	1.46	2.47	0.45
OA	SPP	2.76	3.85	1.67	1.63	2.47	0.78
OA	SQQ	6.45	5.48	7.42	1.56	2.67	0.45
OA	M12	4.87	5.28	4.47	2.37	1.62	3.12
OA	S12	2.28	1.15	3.40	0.55	0.77	0.34
SA	111	5.34	5.27	5.40	2.01	2.12	1.90
SA	S11	2.16	3.39	0.93	1.32	2.07	0.56
SA	222	4.63	4.27	4.98	3.18	3.26	3.10
SA	S22	3.54	2.17	4.91	0.68	0.94	0.41
SA	SPQ	8.13	7.31	8.96	2.22	3.90	0.53
SA	SPP	4.49	7.31	1.67	2.34	3.90	0.78
SA	SQQ	7.22	5.48	8.96	1.60	2.67	0.53
SA	M12	5.13	5.27	4.98	2.61	2.12	3.10
SA	S12	4.15	3.39	4.91	1.24	2.07	0.41
Ground-State TDDFT							
	KS-LR	0.52	0.47	0.57			
	KS-TDA	0.37	0.19	0.56			

All of the calculations were performed using the Q-Chem⁵⁵ and MOLPRO⁵⁶ software packages.

9. RESULTS AND DISCUSSION

9.1. Examples of the Three SF-KS-TDA Assignment Methods: EA, OA, and SA. In section 6, we introduced three assignments methods (EA, OA, and SA) for assigning the excited singlet state from an SF-KS-TDA calculation. In this subsection, we use Be and Ne as examples to illustrate how we used the three assignment methods.

For Be, the states of interest are the valence excited state with the 2s2p configuration and the Rydberg excited state with the 2s3s configuration. Taking a 2s2p_x triplet state as the reference for SF-KS-TDA calculations, we found that all of the states of interest obtained by a collinear GVWN5 calculation are spin-contaminated with $\langle S^2 \rangle \approx 1$, as shown in Table 4. To collect the energy of the 2s2p singlet state, the EA method of assignment method takes the energy of the lowest-energy 2s2p state whether or not it has the same open-shell subspace as the reference. In the present case, this lowest-energy state is a 2p_x α to 2p_y β spin-flip excitation from the 2s2p_x reference triplet. The OA and SA methods need to take the energies of the 2s2p states with the same open-shell subspace as the reference. These two 2s2p states are the states obtained by equal mixing of the pure triplet and pure singlet 2s2p states (this is the situation depicted in the left side of Figure 2); OA takes the

lower-energy 2s2p state, which arises from a 2p_x α to 2p_y β spin-flip excitation of the reference, while SA takes the higher-energy 2s2p state, which arises from a 2s α to 2s β spin-flip excitation. For the 2s3s singlet state, all three assignment methods involve the lowest-energy 2s3s state, which is obtained by changing the 2p_x α spin-orbital of the reference determinant to a 3s β spin-orbital.

The noncollinear SF-KS-TDA using GVWN5 usually can eliminate the spin contamination of states that have the same configuration as the triplet reference. For example, as shown in Table 4, if one uses the 2s3s triplet state of Be as the reference, the noncollinear SF-KS-TDA calculation with GVWN5 produces the pure 2s3s triplet ($\langle S^2 \rangle = 2.0000$) and pure 2s3s singlet ($\langle S^2 \rangle = 0.0155$). On the basis of the way we defined the three assignment methods, all three of them take the pure 2s3s singlet. Similarly, the 2s2p state obtained from SF-KS-TDA calculations using 2s3s as the reference is always spin-contaminated as a result of spin incompleteness, so the lowest-energy 2s2p state is chosen by all assignment methods.

For Ne, we take an example that obtains the states with $\langle S^2 \rangle$ values of $\sim 1-1.5$. We are interested in the 2p⁵3s and 2p⁵3p states of Ne. When the 2p_x²2p_z²2p_y3p_y triplet is used as the reference, the 2p⁵3s state is always spin-contaminated, so the EA, OA, and SA methods of assignment all take the lowest-energy 2p⁵3s state. The lowest-energy 2p⁵3p state obtained from the noncollinear SF-KS-TDA calculation using LRC-

Table 6. Smallest MUE(6) (in eV) of Each Tested Functional for Be Using Collinear and Noncollinear SF-KS-TDA, KS-LR, and KS-TDA

functional	SF-KS-TDA		ground-state TDDFT	
	kernel-assign.-scheme	MUE(6)	method	MUE(6)
GVWNS	C-OA-S12	0.28	KS-LR	0.46
	N-EA-SPQ	0.27	KS-TDA	0.36
PBE	C-OA-S11	0.50	KS-LR	0.60
	N-EA-S12; N-EA/OA/SA-S22	0.40	KS-TDA	0.45
M06-L	C-EA-S11	1.99	KS-LR	0.68
	N-EA/OA-S11	0.58	KS-TDA	0.40
ω B97X	C-EA-S11	1.66	KS-LR	0.33
	N-SA-S22	0.80	KS-TDA	0.21
M06	C-EA-S11	0.31	KS-LR	0.72
	N-OA-S12	0.27	KS-TDA	0.64
M06-2X	C-EA-S11	1.37	KS-LR	0.48
	N-EA/OA-S11	0.57	KS-TDA	0.34
B97-1	C-EA-S11	1.17	KS-LR	0.40
	N-EA/OA-S11	0.54	KS-TDA	0.31
B3PW91	C-EA-S11	0.55	KS-LR	0.52
	N-EA-S12; N-EA/OA/SA-S22	0.30	KS-TDA	0.36
LRC- ω PBE	C-EA-S11	0.43	KS-LR	0.49
	N-EA-S12	0.35	KS-TDA	0.31
LRC- ω PBEh	C-EA-S11	0.57	KS-LR	0.53
	N-EA-S12	0.30	KS-TDA	0.36

ω PBEh is a spin-contaminated state with $\langle S^2 \rangle = 1.0027$ that has different open-shell subspace ($2p_z$ and $3p_y$) from the reference ($2p_y$ and $3p_y$), and EA takes this state as the $2p^5 3p$ singlet state. The two $2p^5 3p$ states with the same open-shell subspace as the reference are the two states with $\langle S^2 \rangle = 1.2161$ and 0.7750 , and they are also spin-contaminated as a result of unequal mixing of the pure singlet and triplet, as shown in the right side of Figure 2. On the basis of the definition of the OA method, OA takes the state with $\langle S^2 \rangle = 1.2161$ as the $2p^5 3p$ singlet because of its $\langle S^2 \rangle$ value in the range 0–1.5 and its relatively lower energy. In contrast, the SA assignment method takes the state with the smaller $\langle S^2 \rangle$ value (0.7750).

9.2. Be Atom. In this subsection, we will mainly report the performance of TDDFT methods for Be. The paper would be too long if we were to go through all of the results for all of the atoms and cations in detail, but we believe it is important to present the results for one atom in detail; the results for the other tested atoms and the cations can be found in the Supporting Information. Then the performance of the methods averaged over all six tested atoms and cations will be reported in subsection 9.3. We chose Be as the example because it is the simplest atom among the six tested atoms and also because the excitations investigated here include both valence and Rydberg excitations of Be, for which the different TDDFT methods often have different accuracies.

Table 5 lists the mean unsigned errors (MUEs) of the KS-LR, KS-TDA, and SF-KS-TDA methods for Be. There are 27 choices for collinear SF-KS-TDA and 27 choices for noncollinear SF-KS-TDA, where the value 27 results from nine schemes times three assignment methods. Each number in Table 5 is averaged over the 10 density functionals. The reader should note that Table 5 summarizes a very large number of calculations; in particular, gathering this data required the assignment of $(27 + 27 + 2) \times 10 = 560$ theoretical spectra. The MUE(60) in Table 5 is the MUE of 60 values obtained by each method; there are 60 values because there are six experimental energy differences ($T_1 - S_0$, $T_2 - S_0$, $S_1 - S_0$, S_2

$- S_0$, $S_1 - T_1$, and $S_2 - T_2$), and 10 functionals. The six energy differences include both valence and Rydberg excitations; MUEV(30) and MUER(30) are the MUEs of the values including only valence excitations ($T_1 - S_0$, $S_1 - S_0$, and $S_1 - T_1$) and only Rydberg excitations ($T_2 - S_0$, $S_2 - S_0$, and $S_2 - T_2$), respectively.

As shown in Table 5, if we consider both valence and Rydberg excitations of Be, the best performance is obtained by KS-TDA [MUE(60) = 0.37 eV], and KS-LR is considerably less accurate than KS-TDA [MUE(60) = 0.52 eV]. No matter how we assign the states (EA, OA, or SA, as explained in section 6 and subsection 9.1), all of the collinear SF-KS-TDA calculations give very large values of MUE(60) (0.91–8.13 eV). The smallest of these values, 0.91 eV, is obtained using the S11 scheme with the energy-based assignment method. Using a noncollinear kernel reduces the errors of SF-KS-TDA calculations by a wide margin compared with using a collinear kernel, with MUE(60) values reduced to 0.51–3.19 eV. The best value, 0.51 eV, is obtained using the S12 scheme, again with energy-based assignment, and this error is even slightly smaller than the error in KS-LR. The wide range of MUE(60) values for the spin-flip methods in Table 5 should make clear, if it was not clear already, why we were so careful to delineate the various possible ways to calculate the energies and assign the states; it makes a tremendous difference!

From Table 5, we can also see that KS-TDA gives a very small error for valence excitations of Be [MUEV(30) = 0.19 eV], while noncollinear SF-KS-TDA calculations with the S22 or S12 schemes (on the basis of the definitions in section 5, these two schemes are the same when only Rydberg excitations of Be are considered) exhibit the best performance for Rydberg excitations: the energy-based and occupation-based assignment methods give MUER(30) = 0.34 eV, while the spin-based assignment scheme gives MUER(30) = 0.41 eV.

From these Be results, we conclude that the performance of SF-KS-TDA calculations, averaged over the 10 functionals, depends strongly on the choice of energy calculation scheme,

the choice of assignment method, and the choice of whether to use a collinear or noncollinear kernel. To further complicate matters, the different functionals prefer different choices for schemes and assignment methods. This latter characteristic may be contrasted to the results for the ground-state TDDFT methods, for which all 10 tested functionals give smaller MUEs for KS-TDA than for KS-LR. Table 6 shows the smallest MUE(6) (in eV) of each tested functional for Be using collinear and noncollinear SF-KS-TDA compared with those using the KS-LR and KS-TDA methods, where MUE(6) is the mean unsigned error of the six values $T_1 - S_0$, $T_2 - S_0$, $S_1 - S_0$, $S_2 - S_0$, $S_1 - T_1$, and $S_2 - T_2$ obtained using that particular functional and method. In Table 6, the SF-KS-TDA methods are labeled as “kernel-assignment method-scheme”, where a collinear kernel is denoted by C and a noncollinear kernel by N. It is seen that for some functionals even collinear SF-KS-TDA can describe both valence and Rydberg excitations of Be well. For example, the C-OA-S12 method with the GVWN5 functional and the C-EA-S11 method with the M06 functional have MUE(6) values of 0.28 and 0.31 eV, respectively. For five of the 10 functionals, in particular GVWN5, PBE, M06, B3PW91, and LRC- ω PBEh, there is a choice of method for SF-KS-TDA calculations that can give better results than both KS-TDA and KS-LR with that functional. It is interesting to note that the ω B97X functional gives the smallest MUE(6) for KS-TDA calculations (0.21 eV) but exhibits the worst performance for noncollinear SF-KS-TDA calculations [MUE(6) = 0.80 eV].

Of course, a method could perform fortuitously well or uncharacteristically poorly if we examine just a single atom, so we performed the same kind of analysis for B^+ , Ne, Na^+ , Mg, and Al^+ , and in the next subsection we will average the performance of the methods over all six tested systems in order to draw more general conclusions.

9.3. Overall Performance Averaged over Three Atoms and Three Cations. The overall performance of KS-LR, KS-TDA, and all 18 SF-KS-TDA schemes is characterized for all six tested systems by MUE(360), which is the mean unsigned error of 360 values: 10 functionals, six systems, and six energy differences per system. The MUE(360) values are plotted as a column chart in Figure 3. The corresponding mean signed errors, MSE(360), are plotted in Figure 5. We also consider MUEV(120), which includes only the valence excitations of the four systems that have valence excitations (Be, B^+ , Mg, and Al^+), and MUER(240), which includes the rest of the excitations (i.e., the Rydberg excitations) for all six systems; these quantities are plotted in Figure 4.

From Figure 3 we can see the following trends:

- (1) Noncollinear SF-KS-TDA calculations always have 2–4 times smaller MUEs than collinear ones.
- (2) The S11, S22, and S12 schemes for SF-KS-TDA always exhibit better performance than the other schemes.
- (3) When a noncollinear kernel is used, no matter which assignment method is used, the S11, S22, and S12 schemes of SF-KS-TDA can give smaller or similar MUE(360) values compared with KS-LR and KS-TDA.
- (4) The energy-based assignment method (EA) gives the smallest MUE(360) values for most SF calculations.

From Figure 4 we can see the following trends:

- (5) Collinear spin-flip methods are less accurate than noncollinear spin-flip methods or conventional TDDFT for both valence and Rydberg excitations.

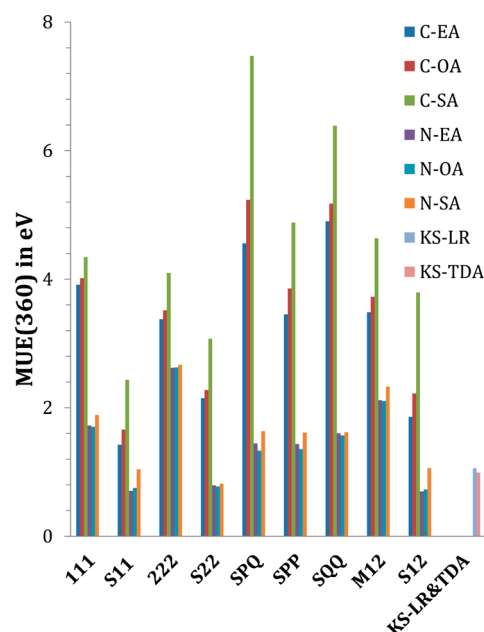


Figure 3. Mean unsigned errors for the 18 SF-KS-TDA methods [schemes 111–S12 with a collinear (C) or noncollinear (N) kernel] using each of the three assignment methods (EA, OA, and SA) and for KS-LR and KS-TDA. The quantity MUE(360) shown in this figure is averaged over 10 functionals, six systems, and six energy differences for each system.

- (6) Noncollinear spin-flip methods are more accurate than conventional TDDFT for Rydberg states.
- (7) Noncollinear spin-flip methods are less accurate than conventional TDDFT for valence states.

From Figure 5, we can see the following trend:

- (8) Conventional TDDFT tends to underestimate the excitation energies, but systematic errors in the spin-flip methods can have either sign, depending on other choices.

Trend (1) can be explained by the observation that the use of a noncollinear kernel usually eliminates the spin contamination to some extent, as shown in the Be and Ne examples in subsection 9.1, and this is probably the main reason that the noncollinear SF-KS-TDA calculations exhibit better performance than collinear ones.

Trend (2), the larger MUE values of the 111, 222, and M12 schemes compared with the corresponding S11, S22, and S12 schemes, indicates that it is preferable to calculate S_0 by RKS, although there might have been an expectation that excitation energies would be more accurate if both S_0 and excited states were calculated consistently by TDDFT or that the ground state would be more accurate if it were explicitly mixed with doubly excited configurations. One reason for the better performance with RKS ground states is that the SF-KS-TDA methods express the S_0 state with orbitals optimized for a triplet. To test whether this is the reason, we can check whether the energy of the S_0 state is usually overestimated.⁵⁷ Figure 6 confirms this; it shows the MSEs of the various functionals for the S_0 state calculated by SF-KS-TDA methods over six systems relative to those obtained by RKS. We can see that most of functionals seriously overestimate the energy of the S_0 state with SF calculations. This explains the negative or less positive

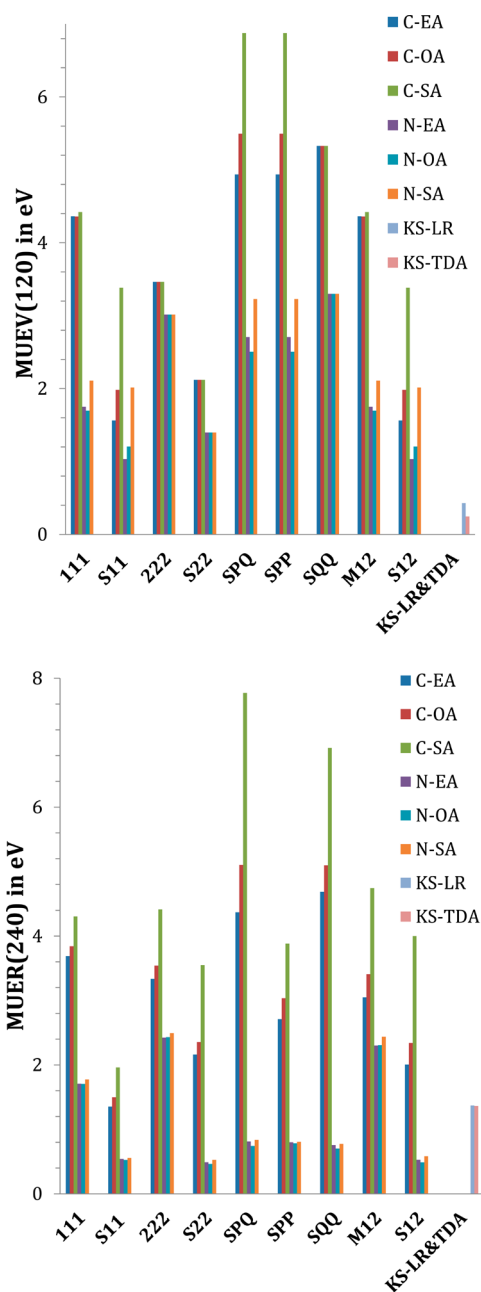


Figure 4. Mean unsigned errors for the 18 SF-KS-TDA methods [schemes 111–S12 with a collinear (C) or noncollinear (N) kernel] using each of the three assignment methods (EA, OA, and SA) and for KS-LR and KS-TDA. The quantity MUEV(120) in the top chart is based on valence excitations, and the quantity MUEV(240) in the bottom chart is based on Rydberg excitations.

MSE(360) values of the 111, 222, and M12 schemes in Figure 5.

A second main reason for the inaccurate S_0 energy obtained using SF is illustrated in Figure 7, which shows the mean $\langle S^2 \rangle$ value of the S_0 state predicted by SF-KS-TDA; comparing Figure 7 to Figure 6 shows that the extremely inaccurate S_0 states often correspond to larger $\langle S^2 \rangle$ values.

The SPQ, SPP, and SQQ schemes, which apply Yamaguchi's formula (eq 9) to project the spin-mixed state, exhibit the worst performance using the collinear kernel, even though they use the S_0 energy obtained by RKS calculations. This is disappointing because in one of our previous papers,⁹ we

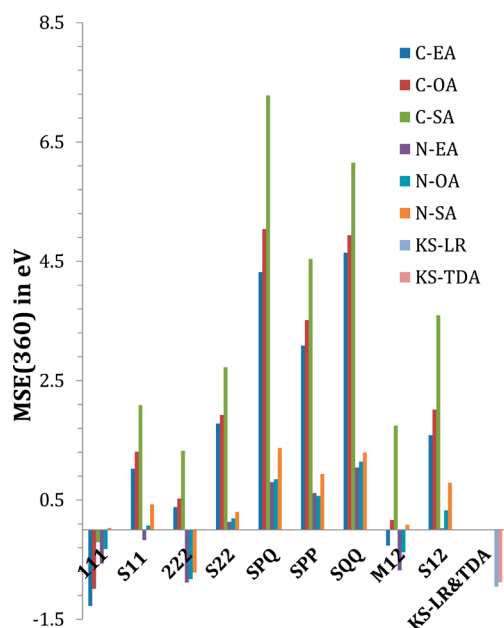


Figure 5. Mean signed errors for the 18 SF-KS-TDA methods [schemes 111–S12 with a collinear (C) or noncollinear (N) kernel] using each of the three assignment methods (EA, OA, and SA) and for KS-LR and KS-TDA. The quantity MSE(360) is averaged over 10 functionals, six systems, and six energy differences for each system.

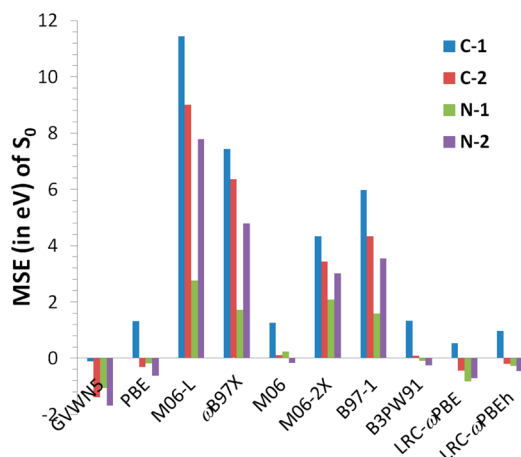


Figure 6. MSEs of six systems for each functional for the S_0 energy calculated using both collinear (C) and noncollinear (N) SF-KS-TDA with the first (1) or second (2) triplet as the reference, compared with the S_0 energy calculated using the RKS method with the corresponding functional.

reported that the SF2 method, which is the present SPQ scheme with a collinear kernel, works well for one particularly important kind of molecular system for some hybrid functionals with $X = 50$ –60. There are, however, three possible reasons for its poorer performance here. The first reason is that most of the excitations investigated in the present work (see Table 1) involve degenerate p orbitals, but there is only one singly occupied p orbital in the reference triplet state; therefore, the spin contamination comes mainly from the spin incompleteness of determinants f – j , which cannot be removed by Yamaguchi's formula, as we mentioned at the end of subsection 2.3. The OA and SA methods of assigning states are supposed to alleviate this type of spin contamination; however, we have shown that MUE(360) and the magnitude of MSE(360) are larger for

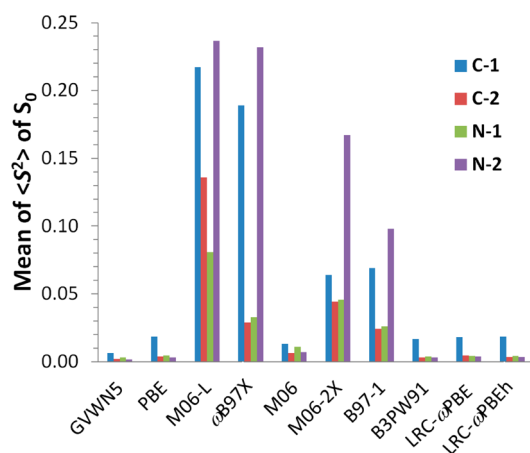


Figure 7. Mean of the $\langle S^2 \rangle$ values of the S_0 states of six systems for each functional calculated using both collinear (C) and noncollinear (N) SF-KS-TDA with the first (1) or second (2) triplet as the reference.

these two assignment methods. Another possible reason why the SF2 method works poorly here is that the singlet states involve mixtures of combinations of determinants of types d and e plus small amounts of higher-energy determinants.

A third possible reason for the poor performance of the SF2 method is that when we use the energy of the triplet reference state for E_T in eq 9, we assume that the triplet reference state ($M_S = 1$) has a similar energy as the triplet state with $M_S = 0$ obtained by spin-flip excitation from the reference state, but this hypothesis is true only if the functional under consideration can predict an accurate energy for virtual β orbitals. However, we noticed that many functionals that are good functionals for the ground state (e.g., M06-L, M06-2X, ω B97X, and B97-1) do not yield accurate virtual β orbitals from UKS calculations of the reference triplet state. We can infer this indirectly from the inaccurate S_0 energy obtained by SF methods in Figure 6, but it can also be confirmed directly by examining the orbitals. Figure 8 plots the Rydberg β orbitals of the $2p^5 3s$ triplet state of Ne

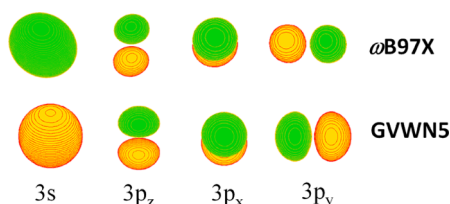


Figure 8. Rydberg β orbitals ($3s$ and $3p$) of the $2p^5 3s$ triplet state of Ne calculated by ω B97X (top; contour value = 0.02 au) and GVWN5 (bottom; contour value = 0.05 au).

($3s\beta$ and $3p\beta$, which are unrelaxed virtual orbitals) obtained by UKS calculations using ω B97X and GVWN5. We can see that ω B97X gives a deformed, ellipsoidal, and tighter (the maximum density is ~ 1.30 atomic units) $3s\beta$ orbital compared with the spherical $3s\beta$ orbital with maximum density of ~ 0.80 atomic units obtained by GVWN5. The $3p\beta$ orbitals of ω B97X are more diffuse (i.e., have more Rydberg character) than those of GVWN5; this is not visually apparent in the figure because (in order to obtain representative plots) a smaller contour value had to be used for the ω B97X orbitals (0.02 atomic units) than for the GVWN5 orbitals (0.05 atomic units).

Because the noncollinear kernel allows mixing of the α and β spin-orbitals, it allows both two-electron-integral exchange and exchange–correlation exchange (eqs 5 and 6) to contribute to SF-KS-TDA excitation energies. We see that the use of the noncollinear kernel ameliorates the performance of the SPQ, SPP, and SQQ schemes, just as it does for the other six SF schemes, and this improvement is slightly larger for SPQ, SPP, and SQQ when Rydberg excitations are considered.

Trend (3), that noncollinear spin-flip calculations are more accurate than conventional TDDFT, results largely because the KS-LR and KS-TDA methods fail badly for Rydberg excitations; on the contrary, the SF-KS-TDA calculations using a noncollinear kernel with the S11, S22, and S12 schemes can describe Rydberg excitations better. The noncollinear spin-flip calculations are sometimes worse than conventional TDDFT for valence excitations (and sometimes better). The worse performance for valence states of SF-KS-TDA compared with KS-LR and KS-TDA was emphasized in a recent study⁵⁸ of valence excitation in molecular systems. The spin contamination introduced by SF-KS-TDA is probably the main reason leading to its failure for valence states. In fact, SF-KS-TDA is more strongly functional-dependent than ground-state TDDFT, and its performance also depends on how it is used. Nevertheless, when averaged over the valence and Rydberg states, the overall performance of noncollinear spin-flip calculations is systematically better than that of conventional TDDFT. It is very important in this regard to keep in mind that in molecules the Rydberg states are often close in energy to valence states and that many valence states have partial Rydberg character; thus, a successful method for molecules should treat both valence and Rydberg states well. The problem is quite serious because the conventional TDDFT method typically underestimates the energies of Rydberg states, increasing the likelihood of spurious mixing with valence states or of misassignments of molecular spectra.

In order to elucidate the other trends, Table 7 lists MUEs and MSEs averaged over the six systems for selected methods. The methods selected for Table 7 include the best noncollinear method for each functional and the conventional KS-TDA results for each functional. Only average results are shown for collinear spin-flip methods because of their poor performance compared with noncollinear methods, and only average results are shown for conventional KS-LR calculations because of their poor performance relative to KS-TDA (the reader can refer to the other tables and to the Supporting Information for more details on collinear spin-flip calculations and KS-LR calculations, but here we are trying to focus the discussion on the more important results). As shown in Table 7, although the smallest MUE for SF-KS-TDA calculations in the present study averaged over the 10 functionals and six systems is 0.70 eV, which is obtained using the noncollinear S12 scheme with the EA assignment method (labeled as N-EA-S12:10 functionals in Table 7), the GVWN5 and M06 functionals, with a noncollinear kernel and the proper choice of assignment method and energy computation scheme, can reduce the MUE by half (MUE = 0.27 eV for N-EA-SPQ:GVWN5 and MUE = 0.33 eV for N-OA-S12:M06). This dependence on the functional for SF methods is stronger for valence excitations than for Rydberg ones. This is illustrated by a comparison of the MUEV of 1.03 eV for the N-EA-S12 method, which is the smallest MUEV for any of the nine collinear methods when only valence excitations are considered and when the results are averaged over the 10 functionals and six systems, with the two

Table 7. Selected MUEs and MSEs (in eV) Averaged over the Six Systems^a

	MUE	MUEV	MUER	MSE	MSEV	MSER
EOM-CCSD	0.09	0.04	0.12	−0.05	−0.01	−0.08
CASPT2	0.24	0.12	0.30	−0.17	0.03	−0.27
CIS	0.77	0.72	0.79	0.11	−0.11	0.21
SF-CIS-EA-SPQ/SPP	0.89	0.78	0.95	−0.59	−0.11	−0.82
TDHF	1.11	1.73	0.80	0.04	−0.29	0.21
N-EA-SPQ:GVWN5	0.27	0.24	0.28	−0.04	0.10	−0.10
N-OA-S12:M06	0.33	0.33	0.33	0.02	0.17	−0.05
N-EA-S12:B3PW91	0.37	0.46	0.32	−0.15	−0.42	−0.02
N-EA-S22:LRC- ω PBE	0.38	0.64	0.25	−0.22	−0.64	0.00
N-EA-S22:LRC- ω PBEh	0.41	0.69	0.27	−0.25	−0.69	−0.03
N-EA/OA-S22:PBE	0.44	0.46	0.44	−0.13	−0.39	0.00
N-EA-S11:M06-2X	0.56	0.78	0.45	−0.04	0.55	−0.34
N-EA-S11:B97-1	0.69	1.54	0.26	0.39	1.43	−0.13
<u>N-EA-S12:10 functionals</u>	<u>0.70</u>	<u>1.03</u>	<u>0.53</u>	<u>0.03</u>	<u>0.23</u>	<u>−0.08</u>
<u>N-OA-S22:10 functionals</u>	<u>0.78</u>	<u>1.40</u>	<u>0.46</u>	<u>0.19</u>	<u>0.42</u>	<u>0.08</u>
N-EA-S11: ω B97X	0.82	1.91	0.28	0.56	1.71	−0.02
N-EA-S11:M06-L	1.03	2.39	0.36	0.75	2.17	0.04
<u>C-EA-S11:10 functionals</u>	<u>1.42</u>	<u>1.56</u>	<u>1.35</u>	<u>1.02</u>	<u>1.24</u>	<u>0.92</u>
KS-TDA:M06-2X	0.64	0.27	0.83	−0.51	0.10	−0.82
KS-TDA: ω B97X	0.80	0.17	1.11	−0.70	−0.02	−1.05
KS-TDA:B97-1	0.82	0.11	1.18	−0.74	0.02	−1.12
KS-TDA:B3PW91	0.86	0.30	1.14	−0.75	0.03	−1.14
<u>KS-TDA:10 functionals</u>	<u>0.99</u>	<u>0.25</u>	<u>1.36</u>	<u>−0.88</u>	<u>0.02</u>	<u>−1.33</u>
KS-TDA: LRC- ω PBEh	0.99	0.34	1.31	−0.86	0.02	−1.30
KS-TDA:GVWN5	1.10	0.17	1.56	−1.03	0.05	−1.56
KS-TDA:M06-L	1.11	0.22	1.56	−0.90	0.14	−1.42
KS-TDA:LRC- ω PBE	1.15	0.36	1.55	−1.01	0.03	−1.53
KS-TDA:M06	1.22	0.24	1.71	−1.18	−0.17	−1.68
KS-TDA:PBE	1.23	0.30	1.70	−1.12	0.04	−1.69
<u>KS-LR:10 functionals</u>	<u>1.06</u>	<u>0.43</u>	<u>1.37</u>	<u>−0.95</u>	<u>−0.19</u>	<u>−1.34</u>

^aThe underlined numbers were obtained by averaging over the 10 tested functionals.

best MUEV values for individual functionals, namely, 0.24 eV for N-EA-SPQ:GVWN5 and 0.33 eV for N-OA-S12:M06. The situation is even more striking for the Rydberg states, where N-EA-S12, which is the best combination averaged over both valence and Rydberg excitations for the 10 functionals, has an average MUER of 0.53 eV, which is significantly larger than the MUER for every one of the 10 functionals (they are all 0.45 eV or less). This comes about, for example, because the best performance for each functional does not result from the same scheme (S11, S12, or S22) and the difference produced by using another scheme can be significant. Therefore, this shows that there is no one combination of assignment method and scheme that works relatively well for all 10 functionals. If we ask for the best method judged by MUER averaged over the 10 functionals, the answer is N-OA-S22, with MUER = 0.46 eV, which is still larger than the value of 0.45 eV mentioned above. (When averaged over both valence and Rydberg excitations, N-OA-S22 gives MUE = 0.78 eV, which is a little higher than N-EA-S12's 0.70 eV.)

Trend (4), that the energy-based assignment method (EA) gives the smallest MUE(360) values for most SF calculations, is reflected in more detail in Table 7 in that the EA method gives the best performance for noncollinear spin-slip calculations for nine of the 10 functionals. The exception is M06, which gets significantly better results with the OA assignment method, in particular an MUE of 0.33 eV versus 0.76 eV for EA. Although spin-based assignment (SA) also seemed like a reasonable choice—maybe even the most reasonable choice—before doing

the statistics, Figure 3 shows that it is worse than the other two assignment methods for all nine noncollinear schemes.

Trends (5) and (6) for Rydberg states, that collinear SF methods do not improve the performance compared with conventional TDDFT but noncollinear spin-flip methods do so in a dramatic fashion, is a major result of the present study. It is well-known that the ground-state TDDFT method usually exhibits much worse performance for Rydberg excitations than for valence excitations because of the incorrect asymptotic behavior of the exchange–correlation potential used.^{12,59} The approximate exchange–correlation functionals usually overestimate the ground-state potential at long range,⁶⁰ and hence, the excitation energies of Rydberg states are often seriously underestimated. This is also observed in the present study, as evidenced by the MSERs, averaged over the 10 functionals, of −1.33 eV for KS-TDA and −1.34 eV for KS-LR. M06-2X is the functional with the smallest MUER (0.83 eV) for ground-state TDDFT calculations, and even in this method, the errors are very systematic (MSE = −0.82 eV).

Some functionals show wildly different performances for valence and Rydberg transitions, as exemplified in a most interesting fashion by the B97-1 functional. Although B97-1 always has a large MUE when we consider valence and Rydberg states together, whether in conventional TDDFT, collinear spin-flip, or noncollinear spin-flip calculations, it performs best for valence states by KS-TDA (MUEV = 0.11 eV) and describes Rydberg states reasonably well by noncollinear SF-KS-TDA calculations (MUER = 0.26 eV for N-EA-S11).

Among the 10 tested functionals, M06-2X performs best for ground-state TDDFT methods, with an MUE of 0.64 eV (for KS-TDA; see Table 7), and is also best for Rydberg states. Although, like all functionals for conventional TDDFT, it is much better for valence states than for Rydberg states, the reason that it is overall the best method for conventional TDDFT is its *relatively* good performance for Rydberg states. This could be hidden in an application to molecules when valence and Rydberg states get mixed.

Although not shown in Table 7, M06-2X is not only the best functional for KS-TDA, it is also best for KS-LR, with an MUE of 0.67 eV. For all 10 functionals, KS-TDA leads to a lower MUE than does KS-LR, with the differences ranging from 0.02 to 0.12 eV.

9.4. Comparison to Wave Function Methods. Although there are many tests of TDDFT methods in the literature, one does not usually have results from wave function theory (WFT) for the identical test suite. In the present study, we calculated wave function results to remedy this. Therefore, Table 7 also lists the MUEs and MSEs obtained by the TDHF, CIS, CASPT2, and EOM-CCSD methods and by the best method for SF-CIS, which involves the EA method for assigning states and the **SPQ** or **SPP** energy calculation scheme.

In contrast to the often-unsatisfactory overall performance of the time-dependent density functional methods, the wave function method EOM-CCSD works relatively well for these cases, giving an MUE of only 0.09 eV. Of course, we should keep in mind that this is an expensive method.

The CASPT2 method, which is also expensive compared with TDDFT but is the most commonly used method for studying photochemistry, has an MUE of 0.24 eV. Surprisingly, several of the functionals give MUE and MSER values for noncollinear calculations that are comparable to or better than those of CASPT2 for Rydberg states.

The MUE for CIS (0.77 eV) is similar to that of N-EA-S12 averaged over the 10 functionals (0.70 eV). SF-CIS is less accurate than CIS. TDHF is very inaccurate for valence states.

10. SUMMARY AND CONCLUDING REMARKS

In the present study, we tested 18 schemes (nine with a collinear kernel and nine with a noncollinear kernel) of spin-flip TDDFT (denoted as SF-KS-TDA); this method uses open-shell triplet states as references. For comparison, we also tested conventional linear-response TDDFT (consistently abbreviated as KS-LR) and Tamm–Dancoff-approximation TDDFT (consistently abbreviated as KS-TDA); these methods use closed-shell ground states as references. The tests were carried out to predict electronic excitation energies, including spin splittings, of six systems, all of which are closed-shell atoms or closed-shell monatomic cations (Be, B⁺, Ne, Na⁺, Mg, and Al⁺). The cases tested in the present study are very hard tests for all TDDFT methods (KS-LR, KS-TDA, and SF-TDDFT), probably because most of the excitations studied involve large density changes that cannot be well-described by most approximate exchange–correlation functionals. However, we did find that GVVNS and M06 perform well for both valence and Rydberg excitations with noncollinear SF-KS-TDA calculations when used with the best choices of energy calculation scheme and assignment method. They have competitive MUE values relative to CASPT2, which is more expensive for small systems and impractically expensive for large ones (whereas the density functional method can be applied to *very* large systems). We note that in the present

study, because only atomic systems were involved, we used an active space for CASPT2 of 5 to 7 active orbitals per atom, which would usually be impractical for studying molecules; thus, the error in using CASPT2 in practical studies could be larger than the error here.

We tested 10 exchange–correlation functionals for all 18 TDDFT methods: GVVNS, PBE, M06-L, ω B97X, M06, M06-2X, B97-1, B3PW91, LRC- ω PBE, and LRC- ω PBEh. The performance of all these TDDFT methods was evaluated by averaging over the ten exchange–correlation functionals and over the six systems. For each system, we considered four excitation energies (two singlet and two triplet) and two singlet–triplet splittings. Thus, the MUE for each TDDFT method is an average of 360 values. We found that using noncollinear SF-KS-TDA is systematically better than using the collinear kernel because it allows mixing of the α and β orbitals, which to some extent reduces spin contaminations introduced by the SF method. We also found that noncollinear SF-KS-TDA is systematically better than ground-state TDDFT for Rydberg states but not for valence states. However, with two of the functionals, GVVNS and M06, we can get good accuracy (MUE \leq 0.33 eV) for both valence and Rydberg states.

Our systematic tests yielded useful information about the best ways to use SF-KS-TDA in practical applications. First, it is best to compute the ground-state energy by a restricted Kohn–Sham (RKS) approximation, not by SF-KS-TDA (which might have been favored if there were some advantage in treating ground and excited states more consistently). Second, it is usually best to assign states entirely on the basis of energy (the EA method), although in one case (M06), it is better to assign them by occupation-based assignment (OA); our results indicate that assigning states mainly on the basis of spin expectation values is not recommended.

We always calculated the triplet-state energies using unrestricted Kohn–Sham theory (UKS). The third practical issue is how to calculate the singlet excited-state energies. When the ground state is calculated using RKS, there are six possible schemes for excited states. With the EA assignment method, the noncollinear schemes **S11**, **S22**, and **S12** of noncollinear SF-KS-TDA have the smallest MUE values for most of the tested functionals. With these three schemes, the absolute energies of S_1 and S_2 are obtained from unprojected noncollinear SF-KS-TDA calculations using T_1 or/and T_2 as the reference. The EA assignment method assigns the lowest-energy state with S_1 (or S_2) configuration character as the energy of S_1 (or S_2) only if this state has $\langle S^2 \rangle = 0$ –1.5; otherwise, another mixed state with a smaller $\langle S^2 \rangle$ value (0–0.5) but usually a higher energy is chosen. GVVNS is an exception, and it performs best with the **SPQ** scheme, which uses Yamaguchi’s spin projection formula to cancel the spin contamination. With these choices, noncollinear GVVNS performs the very best overall, with an MUE of only 0.27 eV. The M06 functional has similar performance when a nonlinear kernel and the OA assignment method are combined with the **S12** energy calculation scheme, yielding an MUE of 0.33 eV. The OA assignment method is very similar to the EA one, but it requires that the dominant determinants in the chosen state have the same open-shell subspace as the triplet reference used in the SF calculations. For the **S11**, **S22**, and **S12** schemes, the choice of which triplet state to use as a reference does not change the MUE by more than 0.1 eV when one uses a noncollinear kernel and the EA or OA assignment method.

For the six cases studied, we found that the ground-state TDDFT methods using the closed-shell ground state as the reference state perform better for valence excitations and that KS-TDA performs better (MUEV = 0.25 eV) than KS-LR (MUEV = 0.43 eV) when averaged over the 10 functionals. For Rydberg excitations, the noncollinear **S12** scheme of SF-KS-TDA with the EA assignment method and the noncollinear **S22** scheme with the OA assignment method perform much better (MUER = 0.53 and 0.46 eV, respectively) than KS-TDA (MUER = 1.36 eV) when averaged over the 10 functionals.

The investigation of the performance of each functional for these TDDFT methods yields the following best choices. B97-1 employed in KS-TDA does best for valence excitations (MUEV = 0.11 eV). LRC- ω PBE employed in noncollinear SF-KS-TDA with scheme **S22** and the EA assignment method has the smallest MUER (0.25 eV). However, if one needs to study both valence and Rydberg excitations in the same spectrum (which is often the case for molecules, where the states often have mixed valence–Rydberg character), N-EA-SPQ:GVWN5 and N-OA-S12:M06 are the best choices. Considering that M06 exhibits much better performance on a broad set of databases for ground-state properties,⁴³ we recommend N-OA-S12:M06 for applications.

■ ASSOCIATED CONTENT

■ Supporting Information

MUEs and MSEs of six values ($T_1 - S_0$, $T_2 - S_0$, $S_1 - S_0$, $S_2 - S_0$, $S_1 - T_1$, and $S_2 - T_2$) of each tested system relative to the experimental data for each tested functional and for each tested method (KS-LR, KS-TDA, SF-KS-TDA, and WFT) and for each scheme and assignment method of the SF method, along with the error and the $\langle S^2 \rangle$ value of the S_0 state obtained by the SF method compared with those obtained by the RKS method. This material is available free of charge via the Internet at <http://pubs.acs.org>.

■ AUTHOR INFORMATION

Corresponding Author

*E-mail: truhlar@umn.edu.

Funding

This material is based upon work supported by the U.S. Department of Energy, Office of Basic Energy Sciences, under Grant DE-SC0008666

Notes

The authors declare no competing financial interest.

■ REFERENCES

- (1) Runge, E.; Gross, E. K. U. *Phys. Rev. Lett.* **1984**, *52*, 997.
- (2) Casida, M. E. In *Recent Advances in Density Functional Methods, Part I*; Chong, D. P., Ed.; World Scientific: Singapore, 1995; p 155.
- (3) Jacquemin, D.; Perpète, E. A.; Ciofini, I.; Adamo, C.; Valero, R.; Zhao, Y.; Truhlar, D. G. *J. Chem. Theory Comput.* **2010**, *6*, 2071 and references therein.
- (4) Tapavicza, E.; Tavernelli, I.; Rothlisberger, U.; Filipi, C.; Casida, M. E. *J. Chem. Phys.* **2008**, *129*, No. 124108.
- (5) Casida, M.; Huix-Rotllant, M. *Annu. Rev. Phys. Chem.* **2012**, *63*, 287.
- (6) (a) Minezawa, N.; Gordon, M. S. *J. Phys. Chem. A* **2009**, *113*, 12749. (b) Minezawa, N.; Gordon, M. S. *J. Phys. Chem. A* **2011**, *115*, 7901.
- (7) Curchod, B. F. E.; Rothlisberger, U.; Tavernelli, I. *ChemPhysChem* **2013**, *14*, 1314.
- (8) Tapavicza, E.; Bellchambers, G. D.; Vincent, J. C.; Furche, F. *Phys. Chem. Chem. Phys.* **2013**, *15*, 18336.
- (9) Xu, X.; Gozem, S.; Olivucci, M.; Truhlar, D. G. *J. Phys. Chem. Lett.* **2013**, *4*, 253.
- (10) Hirata, S.; Head-Gordon, M. *Chem. Phys. Lett.* **1999**, *314*, 291.
- (11) Dreuw, A.; Head-Gordon, M. *Chem. Rev.* **2005**, *105*, 4009.
- (12) Levine, B. G.; Quenneville, J.; Martinez, T. J. *Mol. Phys.* **2006**, *104*, 1039.
- (13) Li, S. L.; Marenich, A. V.; Xu, X.; Truhlar, D. G. *J. Phys. Chem. Lett.* **2014**, *5*, 322.
- (14) Starcke, J. H.; Wormit, M.; Schirmer, J.; Dreuw, A. *Chem. Phys.* **2006**, *329*, 39.
- (15) Shao, Y.; Head-Gordon, M.; Krylov, A. I. *J. Chem. Phys.* **2003**, *118*, 4807.
- (16) (a) Wang, F.; Ziegler, T. *J. Chem. Phys.* **2004**, *121*, 12191. (b) Wang, F.; Ziegler, T. *J. Chem. Phys.* **2005**, *122*, No. 074109. (c) Wang, F.; Ziegler, T. *Int. J. Quantum Chem.* **2006**, *106*, 2545.
- (17) Casida, M. E. *J. Mol. Struct.: THEOCHEM* **2009**, *914*, 3 and references therein.
- (18) Hohenberg, P.; Kohn, W. *Phys. Rev.* **1964**, *136*, B864.
- (19) Van Leeuwen, R. *Int. J. Mod. Phys. B* **2001**, *15*, 1969.
- (20) (a) Eshring, H.; Servedio, V. D. P. *J. Comput. Chem.* **1999**, *20*, 23. (b) van Wullen, C. *J. Comput. Chem.* **2002**, *23*, 227.
- (21) Wang, F.; Liu, W. *J. Chin. Chem. Soc. (Taipei)* **2003**, *50*, 597.
- (22) Bernard, Y. A.; Shao, Y.; Krylov, A. I. *J. Chem. Phys.* **2012**, *136*, No. 204103.
- (23) Gao, J.; Lu, W.; Song, B.; Liu, C. *J. Chem. Phys.* **2004**, *121*, 6658.
- (24) (a) Sears, J. S.; Sherrill, D.; Krylov, A. I. *J. Chem. Phys.* **2003**, *118*, 9084. (b) Casanova, D.; Head-Gordon, M. *J. Chem. Phys.* **2008**, *129*, No. 064104.
- (25) (a) Yamaguchi, K.; Takahara, Y.; Fueno, T. In *Applied Quantum Chemistry*; Smith, V. H., Jr., Schaefer, H. F. III, Morokuma, K., Eds.; D. Reidel: Boston, 1986; pp 155–184. (b) Caballol, R.; Castell, O.; Illas, F.; Moreira, I. d. P. R.; Malrieu, J. P. *J. Phys. Chem.* **1997**, *101*, 7860. (c) Shoji, M.; Koizumi, K.; Kitagawa, Y.; Kawakami, T.; Yamanaka, S.; Okumura, M.; Yamaguchi, K. *Chem. Phys. Lett.* **2006**, *432*, 343.
- (26) http://physics.nist.gov/PhysRefData/ASD/levels_form.html (accessed Dec 5, 2013).
- (27) (a) Dirac, P. A. M. *Proc. Cambridge Philos. Soc.* **1930**, *26*, 376. (b) Gáspár, R. *Acta Phys. Acad. Sci. Hung.* **1954**, *3*, 263. (c) Gáspár, R. *Acta Phys. Acad. Sci. Hung.* **1974**, *35*, 213. (d) Vosko, S. H.; Wilk, L.; Nusair, M. *Can. J. Phys.* **1980**, *58*, 1200.
- (28) Perdew, J. P.; Burke, K.; Ernzerhof, M. *Phys. Rev. Lett.* **1996**, *77*, 3865.
- (29) Becke, A. D. *J. Chem. Phys.* **1993**, *98*, 5648.
- (30) Hamprecht, F. A.; Cohen, A.; Tozer, D. J.; Handy, N. C. *J. Chem. Phys.* **1998**, *109*, 6264.
- (31) Henderson, T. M.; Janesko, B. G.; Scuseria, G. E. *J. Chem. Phys.* **2008**, *128*, No. 194105.
- (32) Rohrdanz, M. A.; Martins, K. M.; Herbert, J. M. *J. Chem. Phys.* **2009**, *130*, No. 054112.
- (33) Chai, J.; Head-Gordon, M. *J. Chem. Phys.* **2008**, *128*, No. 084106.
- (34) Zhao, Y.; Truhlar, D. G. *J. Chem. Phys.* **2006**, *125*, No. 194101.
- (35) Zhao, Y.; Truhlar, D. G. *Theor. Chem. Acc.* **2008**, *120*, 215.
- (36) Zhao, Y.; Truhlar, D. G. *Acc. Chem. Res.* **2008**, *41*, 157.
- (37) Tekarli, S. M.; Drummond, M. L.; Williams, T. G.; Cundari, T. R.; Wilson, A. K. *J. Phys. Chem. A* **2009**, *113*, 8607.
- (38) Zhang, W.; Truhlar, D. G.; Tang, M. *J. Chem. Theory Comput.* **2013**, *9*, 3965.
- (39) Li, R.; Zheng, J.; Truhlar, D. G. *Phys. Chem. Chem. Phys.* **2010**, *12*, 12697.
- (40) Peverati, R.; Truhlar, D. G. *Phys. Chem. Chem. Phys.* **2012**, *14*, 11363.
- (41) Isegawa, M.; Peverati, R.; Truhlar, D. G. *J. Chem. Phys.* **2012**, *137*, No. 244104.
- (42) Isegawa, M.; Truhlar, D. G. *J. Chem. Phys.* **2013**, *138*, No. 134111.
- (43) Peverati, R.; Truhlar, D. G. *Philos. Trans. R. Soc., A* **2014**, *372*, No. 20120476.
- (44) Pople, J. A. *Rev. Mod. Phys.* **1998**, *71*, 1267.

- (45) Ciofini, I.; Adamo, C. *J. Phys. Chem. A* **2007**, *111*, 5549.
- (46) Yang, K.; Peverati, R.; Truhlar, D. G.; Valero, R. *J. Chem. Phys.* **2011**, *135*, No. 044118.
- (47) Dunning, T. H., Jr. *J. Chem. Phys.* **1989**, *90*, 1007.
- (48) Woon, D. E.; Dunning, T. H., Jr. *J. Chem. Phys.* **1993**, *98*, 1358.
- (49) <https://bse.pnl.gov/bse/portal> (accessed Dec. 17, 2013).
- (50) Jorgensen, P.; Simons, J. *Second Quantization-Based Methods in Quantum Chemistry*; Academic: New York, 1981; pp 144–148.
- (51) del Bene, J.; Ditchfield, R.; Pople, J. A. *J. Chem. Phys.* **1971**, *55*, 2236.
- (52) Krylov, A. I. *Chem. Phys. Lett.* **2002**, *350*, 522.
- (53) (a) Wernel, H.-J. *Mol. Phys.* **1996**, *89*, 645. (b) Celani, P.; Wernel, H.-J. *J. Chem. Phys.* **2000**, *112*, 5546.
- (54) (a) Emrich, K. *Nucl. Phys. A* **1981**, *351*, 379. (b) Sekino, H.; Bartlett, R. J. *Int. J. Quantum Chem., Symp.* **1984**, *18*, 255. (c) Geertsen, J.; Rittby, M.; Bartlett, R. J. *Chem. Phys. Lett.* **1989**, *164*, 57.
- (55) Kong, J.; White, C. A.; Krylov, A. I.; et al. *J. Comput. Chem.* **2000**, *21*, 1532.
- (56) (a) Wernel, H.-J.; Knowles, P. J.; Knizia, G.; Manby, F. R.; Schütz, M. *Wiley Interdiscip. Rev.: Comput. Mol. Sci.* **2012**, *2*, 242. (b) Wernel, H.-J.; Knowles, P. J.; Knizia, G.; Manby, F. R.; Schütz, M.; Celani, P.; Korona, T.; Lindh, R.; Mitrushenkov, A.; Rauhut, G.; Shamasundar, K. R.; Adler, T. B.; Amos, R. D.; Bernhardsson, A.; Berning, A.; Cooper, D. L.; Deegan, M. J. O.; Dobbyn, A. J.; Eckert, F.; Goll, E.; Hampel, C.; Hesselmann, A.; Hetzer, G.; Hrenar, T.; Jansen, G.; Köppl, C.; Liu, Y.; Lloyd, A. W.; Mata, R. A.; May, A. J.; McNicholas, S. J.; Meyer, W.; Mura, M. E.; Nicklass, A.; O'Neill, D. P.; Palmieri, P.; Peng, D.; Pflüger, K.; Pitzer, R.; Reiher, M.; Shiozaki, T.; Stoll, H.; Stone, A. J.; Tarroni, R.; Thorsteinsson, T.; Wang, M. *MOLPRO: A Package of ab Initio Programs*, version 2012.1; <http://www.molpro.net> (accessed Feb 13, 2014).
- (57) Huix-Rotllant, M.; Natarajan, B.; Ipatov, A.; Muhavini Wawire, C.; Deutsch, T.; Casida, M. E. *Phys. Chem. Chem. Phys.* **2010**, *12*, 12811.
- (58) Isegawa, M.; Truhlar, D. G. *J. Chem. Phys.* **2013**, *138*, No. 134111.
- (59) Casida, M. E.; Jamorski, C.; Casida, K. C.; Salahub, D. R. *J. Chem. Phys.* **1998**, *108*, 4439.
- (60) Gross, E. K. U.; Maitra, N. T. In *Fundamentals of Time-Dependent Density Functional Theory*; Marques, M. A. L., Maitra, N. T., Nogueira, F. M. S., Gross, E. K. U., Rubio, A., Eds.; Lecture Notes in Physics, Vol. 837; Springer: Berlin, 2012; pp 53–99.